Diurnal Variations of Global Thunderstorms and Electrified Shower Clouds and Their Contribution to the Global Electrical Circuit

CHUNTAO LIU

Department of Atmospheric Sciences, University of Utah, Salt Lake City, Utah

EARLE R. WILLIAMS

Parsons Laboratory, Massachusetts Institute of Technology, Cambridge, Massachusetts

EDWARD J. ZIPSER

Department of Atmospheric Sciences, University of Utah, Salt Lake City, Utah

GARY BURNS

Australian Antarctic Division, Australian Government, Kingston, Tasmania, Australia

(Manuscript received 13 July 2009, in final form 21 August 2009)

ABSTRACT

The long-standing mainstay of support for C. T. R. Wilson's global circuit hypothesis is the similarity between the diurnal variation of thunderstorm days in universal time and the Carnegie curve of electrical potential gradient. This rough agreement has sustained the widespread view that thunderstorms are the ''batteries'' for the global electrical circuit. This study utilizes 10 years of Tropical Rainfall Measuring Mission (TRMM) observations to quantify the global occurrence of thunderstorms with much better accuracy and to validate the comparison by F. J. W. Whipple 80 years ago. The results support Wilson's original ideas that both thunderstorms and electrified shower clouds contribute to the DC global circuit by virtue of negative charge carried downward by precipitation. First, the precipitation features (PFs) are defined by grouping the pixels with rain using 10 years of TRMM observations. Thunderstorms are identified from these PFs with lightning flashes observed by the Lightning Imaging Sensor. PFs without lightning flashes but with a 30-dBZ radar echo-top temperature lower than −10°C over land and −17°C over ocean are selected as possibly electrified shower clouds. The universal diurnal variation of rainfall, the raining area from the thunderstorms, and possibly electrified shower clouds in different seasons are derived and compared with the diurnal variations of the electric field observed at Vostok, Antarctica. The result shows a substantially better match from the updated diurnal variations of the thunderstorm area to the Carnegie curve than Whipple showed. However, to fully understand and quantify the amount of negative charge carried downward by precipitation in electrified storms, more observations of precipitation current in different types of electrified shower clouds are required.

1. Introduction

This study is concerned with an examination of a 10-yr satellite database from the Tropical Rainfall Measuring Mission (TRMM) (Kummerow et al. 1998) toward understanding the physical origins of the global circuit of atmospheric electricity. The study is motivated by a long-standing discrepancy between two climatological representations of global circuit behavior and shown together in Fig. 1: the Carnegie curve (Israel 1973) of fair weather atmospheric electricity and the variation in thunder area for the world (Whipple 1929). The Carnegie curve represents the integration of thousands of measurements of the earth's fair weather electric field in universal time over the world's oceans where the planetary boundary layer is relatively free of pollution. The approximate representativeness of the Carnegie curve for individual days is substantiated by measurements of the ionospheric potential (Markson et al. 1999; Markson 2007), a quantity

Corresponding author address: Dr. Chuntao Liu, Department of Atmospheric Sciences, University of Utah, 135 S 1460 E, Rm. 819, Salt Lake City, UT 84112–0110.
E-mail: liu.c.t@utah.edu

DOI: 10.1175/2009JAS3248.1

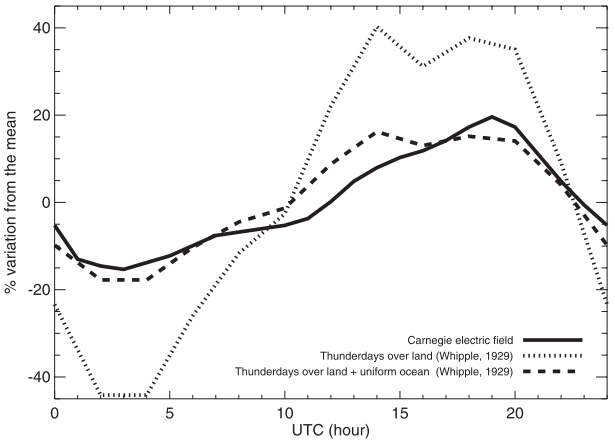

FIG. 1. The diurnal variations of the electric field over tropical ocean (the Carnegie curve) (solid line), global thunder days over land estimated by Whipple (1929) (dotted line), and global thunder days after superimposing an imagined flat diurnal distribution of oceanic thunderstorms (dashed line).

generally regarded as the most reliable measure of the DC global circuit (Williams 2009). The variation of thunder area in Fig. 1 is based on a compilation of thunder day reports from surface meteorological stations worldwide (Whipple 1929) extending over many years and so on that basis is expected to be climatologically representative. We are unaware of global thunder day analysis on individual days, but a consistent day-to-day behavior in global lightning activity on the diurnal time scale is supported by continuous measurements of the intensity of the earth's Schumann resonances (Williams and Sátori 2004).

The diurnal curves in Fig. 1 are often held up in support of the global circuit hypothesis (Wilson 1920) that worldwide electrified weather is maintaining the ~240-kV ionospheric potential and negative charge on the earth. However, these curves differ quantitatively in two key respects: 1) The amplitude variation of the thunder area curve over land is more than twice that of the Carnegie curve. To compensate for this, a uniform diurnal contribution from oceans was assumed that provided a better match to the Carnegie curve from an era when the diurnal variation of oceanic thunderstorms was largely unknown (Whipple 1929). 2) The maximum in the thunder day curve coincides with afternoon thunderstorms in Africa (1400–1500 UTC), whereas the Carnegie curve is maximum when afternoon storms in South America are active (1900–2000 UTC). These discrepancies have been revisited on multiple occasions (Whipple 1929; Pierce 1958; Hill 1971; Williams and Heckman 1993; Kartalev et al. 2006; Bailey et al. 2007; Williams 2009), but the early work on the problem by C. T. R. Wilson and the possibly important role of convective storms not producing thunder both warrant revisitation here.

Early in his foray into atmospheric electricity, Wilson (1903) speculated that the descent of negatively charged precipitation served to maintain the global circuit. In the formulation of his global circuit hypothesis after many subsequent years of thunderstorm investigation, Wilson (1920, p. 112) gave equal attention to thunderclouds and electrified shower clouds as ''batteries'' for the global circuit. In his words:

''A thundercloud or shower-cloud is the seat of the electromotive force which must cause a current to flow through the cloud between the earth's surface and the upper atmosphere ... In shower-clouds in which the potentials fall short of what is required to produce lightning discharges, there is no reason to suppose that the vertical currents are of an altogether different order of magnitude.''

When Whipple (1929) embarked on a test of Wilson's global circuit ideas (in consultation with Wilson), Whipple had a measure of global thunderstorms in the thunder day statistics recently compiled by Brooks (1925). However, no measure of electrified shower clouds was then available. Whipple's well-known test in 1929 (shown in Fig. 1) has left the impression subsequently that Wilson had considered only thunderstorms as batteries, and this notion is still prevalent in the modern literature (Wallace and Hobbs 1977; Williams 1988; Bering et al. 1998; Holzworth et al. 2005). Recent aircraft measurements of the electric field over convective clouds (Mach et al. 2009, 2010) provide firm evidence for the existence of electrified shower clouds that supply current to the global circuit, with predominantly the same polarity as that for thunderstorms (Blakeslee et al. 1989). The simultaneous observation of the vertical structure of precipitation and lightning with the TRMM satellite enable a global climatological study of thunderstorms and electrified shower clouds, and thereby a more comprehensive examination of Wilson's (1920) original hypothesis. The Carnegie curve in Fig. 1 will remain an important benchmark in testing the hypotheses.

The TRMM, launched in December 1997, has both a Precipitation Radar (PR) to measure the surface rainfall and the vertical structure of precipitation and the Lightning Imaging Sensor (LIS) to detect lightning flashes and verify the presence of thunderstorms. With 10 years of observations, the diurnal variation of rainfall and thunderstorm area in universal time can be summarized with a global coverage over the latitude range 35°S to 35°N. Abundant evidence is now available that strong electrification in convective clouds requires the presence of precipitation in the ice phase. For purposes of this study and the strategic use of TRMM satellite observations, it is valuable to consider three classes of convective precipitation ordered by the vertical development

of precipitation radar echoes relative to the 0°C isotherm: 1) shallow clouds whose radar echoes are confined below the height of the 0°C isotherm and whose precipitation is entirely liquid phase, otherwise called ''warm rain clouds;'' 2) transitional clouds whose radar echoes extend above the height of the 0°C isotherm and in which mixed phase processes able to produce electric fields in the range of 10^2 to $\sim 10^6$ V m^{-1}, but insufficiently vigorous to produce lightning, otherwise called ''electrified shower clouds;'' and 3) deep clouds whose increased vertical development above the height of 0°C enables a mature mixed phase microphysics and the development of lightning, otherwise called ''thunderstorms.'' Later, we further distinguish category 2 by reserving the designation of electrified shower clouds for the important subset of category 2 with strong radar echoes in the mixed phase region.

The organization of the paper is as follows: First, the precipitation features are defined from 10 years of TRMM observations. Then the thunderstorms and electrified shower clouds are identified using TRMM LIS flash observations and the thermodynamic environment from National Centers for Environmental Prediction (NCEP) reanalysis. Last, the diurnal variations of rainfall from thunderstorms and electrified shower clouds in universal time are generated and compared to the diurnal variations of the fair weather electric field for various seasons.

2. Data and method

The TRMM satellite has a non-sun-synchronous 35° inclination orbit covering the tropics and subtropics, with instruments for observing precipitation, clouds, and lightning (Kummerow et al. 1998). Given enough observation time, TRMM data provide detailed information about the diurnal cycles of precipitation and clouds (Negri et al. 2002; Nesbitt and Zipser 2003; Liu and Zipser 2008). This study uses the TRMM Precipitation and Cloud Feature (PF) database created from 10 years (1998–2007) of TRMM observations (Liu et al. 2008). The specific database used for this study includes nearly one hundred million PFs defined by grouping the contiguous pixels with near-surface rain observed by the TRMM Precipitation Radar. For each one of these PFs, the geographical center location, rain volume, flash counts, and the maximum PR echo tops are summarized. The rainfall estimates and PR echo tops are taken from the TRMM 2A25 (Iguchi et al. 2000) and 2A23 (Awaka et al. 1998) products. To provide the thermodynamic environment for these PFs, vertical profiles of temperature, geopotential heights for each PF with more than four PR pixels (>75 km^2) are interpolated from 6-hourly NCEP reanalysis data (Kistler et al. 2001). Although there are nearly three-quarters of PFs with less than four PR pixels, their total contribution to rainfall is less than 5% over 35°S–35°N. To control the data volume for easy access, the profiles for these PFs are not derived and saved. Liu et al. (2008) have described this PF database in detail.

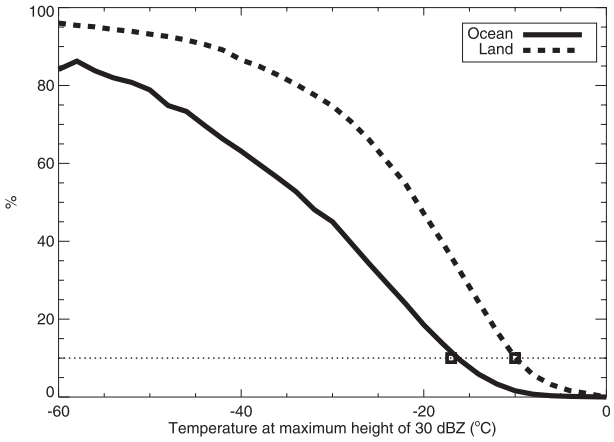

FIG. 2. Probability of PFs with lightning vs temperature of 30-dBZ echo top of PFs over 35°S–35°N land and ocean during 1998–2007. The result is consistent with Cecil et al. 2005.

Thunderstorms are easily identified as PFs with LIS-documented lightning flashes. It should be noted that a PF with lightning can range in size from a single-cell storm to a large mesoscale convective system (MCS) that could contain dozens of individual storm cells, some with lightning and some without. Mach et al. (2009) have reported that about one-third of storms observed by airborne instruments during 12 years had significant electric fields but without lightning, but their statistics are affected by their sampling strategy with the overflying aircraft. As stated in the introduction, the electrified shower clouds are expected to exhibit a vertical development of radar reflectivity intermediate between warm rain shower clouds and full-fledged LIS-observed thunderclouds. The question is how to specify the electrified shower clouds. It is clear that not all transitional clouds whose radar echoes extend to a height above the 0°C isotherm are equally important in producing the electric field. Here we select the electrified shower clouds likely having a large electric field contribution. One approach is to assume that these electrified shower clouds share some characteristics with thunderstorms. For example, Fig. 2 shows the probability of PFs with lightning by their temperature of 30-dBZ echo top generated from 10 years of TRMM PF data. About 10% of land PFs (geographical center locations over land) with 30-dBZ echo top temperature ($T_{30\mathrm{dB}Z}$) below −10°C have lightning. About 10% of oceanic PFs (geographical center locations over ocean) with $T_{30\mathrm{dB}Z}$

below −17°C have lightning. These criteria are consistent with the analysis using three years of TRMM observations by Cecil et al. (2005). Using 10% probability, we may arbitrarily define the electrified shower clouds (without lightning) by two steps. First, the temperature of the maximum height of 30 dBZ for each PF > 75 km^2 is derived from the NCEP vertical profiles of temperature and geopotential heights. Then the electrified shower clouds are selected by PFs with $T_{30\text{dB}Z} < -10$°C over land and PFs with $T_{30\text{dB}Z} < -17$°C over ocean, and without any flash. Note that this definition is rough and arbitrary. The PFs with size <75 km^2 are not included as candidates for electrified shower clouds. Even though three- quarters of PFs are <75 km^2, only 0.02% of them exhibit lightning. Most of them are ''warm'' clouds (Liu and Zipser 2009) and contribute less than 5% of rainfall globally (Table 1).

To generate diurnal variations of thunderstorms and electrified shower clouds in UTC time, first the rain volume and flash counts from 10 years of PFs, thunderstorms, and electrified shower clouds are accumulated in 1° × 1° grids and in 1-h bins of universal time over the latitude interval 35°S–35°N. By virtue of its low inclination orbit, TRMM samples with higher frequency over the subtropics than over the tropics, especially in the latitude range 33°–35°N and S. It is important to remove this sampling bias before generating the diurnal variations of rain volume and flashes; all TRMM data in this paper have been so corrected. Last, the diurnal variations of these parameters are generated by first summing all bias-corrected parameters from all grids for each hour bin, then dividing by the mean values from 24 bins, one for each UTC hour. This procedure yields a relative diurnal variation in UTC time, suitable for comparison with the relative variation of the electric field derived from the Carnegie curve (Israel 1973).

Another important consideration is the ±35° latitude restriction for the intended global analysis. Thunderstorms and electrified shower clouds at higher latitudes also contribute to the global circuit. Appeal to lightning observations made with the Optical Transient Detector (OTD), sampling from the Arctic to Antarctica, suggest that this higher-latitude contribution is minor. It has been confirmed that LIS misses about 11.6% of lightning annually, 10.2% in the Northern Hemisphere (NH), and 1.4% in the Southern Hemisphere (SH) (Bailey et al. 2006). This provides some assurance that conclusions drawn on the basis of the TRMM domain are globally representative.

TABLE 1. Percentages of population, rain area, and rainfall by category of precipitation feature (PF). These include thunderstorms (PFs with flashes), electrified shower clouds (see text), all nonelectrified PFs with size greater than 75 km^2, and all PFs with size less than 75 km^2 over 35°S–35°N land and ocean from 10 years (1998–2007) of TRMM observations. The mean annual rainfall is retrieved from TRMM PR observations by using the TRMM 2A25 algorithm (Iguchi et al. 2000).

	35°S–35°N	Land	Ocean
Mean 35°S–35°N annual rainfall (mm/unit area/yr)	936	870	961
All PFs			
Population	100	19.13	80.87
Rain area	100	24.44	75.56
Rainfall	100	25.17	74.83
Thunderstorms (PFs with flashes)			
Population	0.61	0.45	0.16
Rain area	17.27	9.24	8.03
Rainfall	25.34	13.27	12.07
Electrified shower clouds $T_{30\text{dB}Z} < -10$°C over land; $T_{30\text{dB}Z} < -17$°C over ocean			
Population	0.53	0.34	0.19
Rain area	10.37	2.84	7.53
Rainfall	14.34	3.46	10.88
Nonelectrified PFs >75 km^2			
Population	24.47	4.23	20.23
Rain area	63.68	10.85	52.84
Rainfall	55.40	7.76	47.64
PFs < 75 km^2			
Population	74.39	14.11	60.28
Rain area	8.68	1.51	7.16
Rainfall	4.92	0.68	4.24

3. Results

More than 82 million PFs have been evaluated with these classification criteria from 10 years of TRMM observations over 35°S–35°N, with the finding that 0.43 million PFs are classified as electrified shower clouds and 0.50 million PFs are classified as thunderstorms. In this section, some statistics of these systems and diurnal variations of rain volume and flash counts from them are presented and discussed.

a. Occurrence of rainfall from thunderstorms and electrified shower clouds

The statistics of the PF populations, rainfall and rain area of PFs, electrified shower clouds, and thunderstorms are listed in Table 1. Of all PFs, there are more with geographical center locations over ocean (80.9) than over land (19.1) because of the larger area of oceanic coverage in the tropics and subtropics. Thunderstorms are relatively rare among the populations of precipitating clouds, with only one out of 200 PFs exhibiting flashes (0.6%). Because these thunderstorms may range

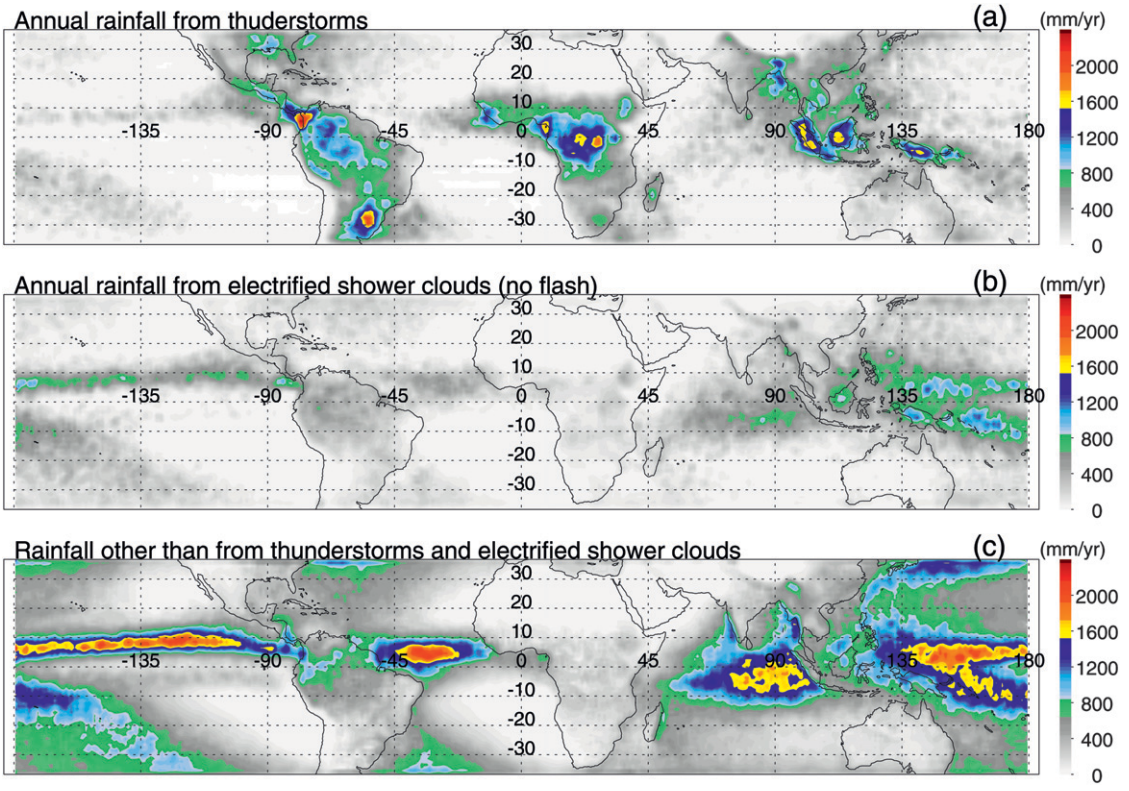

FIG. 3. Mean annual rainfall (a) from thunderstorms (PFs with at least one flash) and (b) from electrified shower clouds, defined by PFs with size >75 km^2, no lightning, $T_{30dBZ} < -10$°C over land and $T_{30dBZ} < -17$°C over ocean. (c) Rainfall other than from thunderstorms and electrified shower clouds. All panels are calculated using 10 years (1998–2007) of TRMM observations.

in size from 75 km^2 upward to large mesoscale systems, they contribute 25% of total rainfall: 13% over land and 12% over ocean. It is possible that the storms with a flash rate lower than the TRMM minimum detectable flash rate (~0.3–0.5 flashes min^{-1}) are not categorized as thunderstorms here. However, they may be included in the 0.53% of PFs identified as electrified shower clouds. These electrified shower clouds contribute 15% of total rainfall: 4% over land and 11% over ocean. Most (nearly 99%) of the PFs do not fall into either of these two electrified cloud categories. This larger population of PFs without electrified cells contributes 60% of total precipitation over 35°S–35°N, about one-third (8.4% out of 25.2%) of precipitation over land and close to two-thirds (51.9% out of 74.8%) of precipitation over oceans.

The geographical distribution of rainfall from thunderstorms, electrified shower clouds, and nonelectrified shower clouds (the remainder of the rainfall) is shown in Fig. 3. Thunderstorms contribute a large amount of rainfall over land, including some heavy rainfall regions over central Africa, Argentina, Panama, and the tropical Maritime Continent (MC) (Fig. 3a). Although the number of PFs categorized as electrified shower clouds over land exceeds that over ocean (0.34% versus 0.19% over oceans, Table 1), they contribute more rainfall over oceans (~10.9%) than over land (~3.5%).

It is clear that nonelectrified rainfall dominates the total rainfall over oceans (Fig. 3c). Over the Amazon and the Maritime Continent, some noticeable contributions of rainfall from nonelectrified showers are evident. Comparing Figs. 3a and 3c, nearly all rainfall over Central Africa, Argentina, and the southern United States is from thunderstorms.

b. Carnegie curve versus rainfall in thunderstorms and electrified shower clouds

Figure 4 shows that the diurnal variation of total rainfall in universal time over 35°S–35°N has a consistent phase with the Carnegie curve, but with substantially lower amplitude. This is because nearly 75% of all rainfall is over ocean, which has a weaker diurnal cycle. The diurnal variation of rainfall over ocean has a substantially smaller amplitude (10% versus 30%) than the Carnegie curve. However, the diurnal variation of rainfall over land, which includes the contributions of PFs

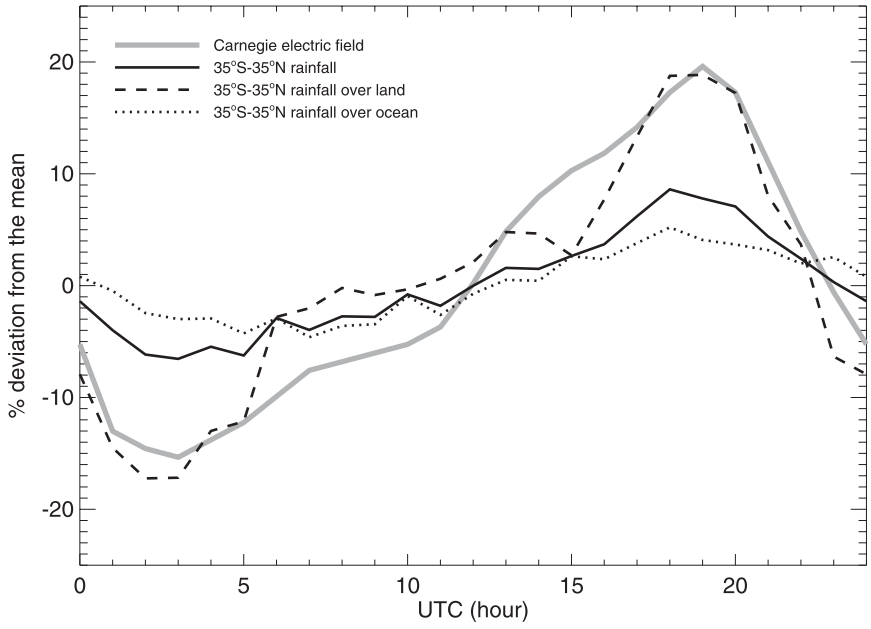

FIG. 4. The Carnegie curve (gray curve) and the diurnal variations of total rainfall (black solid) within 35°S–35°N over land (dashed) and over ocean (dotted).

categorized as thunderstorms and electrified shower clouds, has a similar amplitude. Furthermore, it has an even better consistency with the 0300 UTC minimum phase of the Carnegie curve than that of the thunderstorm rainfall (Fig. 5). The main difference from the diurnal variation of rainfall over land to the Carnegie curve is higher values between 0600 and 1000 UTC when the Maritime Continent is most convectively active (Whipple 1929). The evidence (Table 2) that about 60% of the rainfall over land is delivered by PFs categorized as thunderstorms and electrified shower clouds helps to explain the similarity of rainfall over land to the Carnegie curve.

Figure 5 shows the diurnal variation of rainfall from thunderstorms. In general, the diurnal variation of thunderstorm rainfall has an amplitude close to that of the

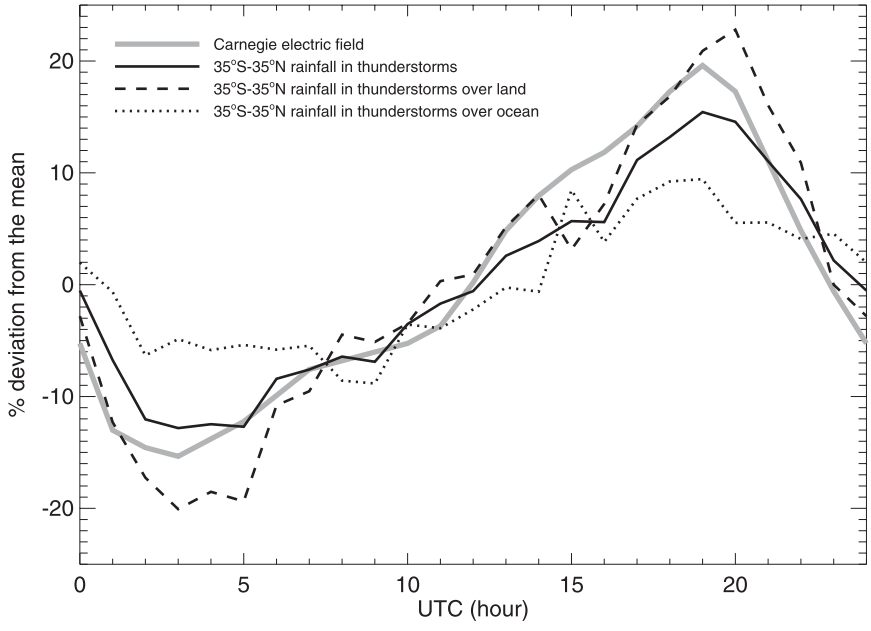

FIG. 5. As in Fig. 4 but for thunderstorms.

TABLE 2. The maximum and minimum phases and amplitudes of diurnal variation of electric field, flash counts, and rainfall inside electrified shower clouds and thunderstorms over tropical and subtropical land and ocean (35°S–35°N). Here electrified shower clouds are defined as precipitation features (PFs) with maximum PR echo-top temperature colder than −10°C over land and −17°C over ocean (see text), where total phase difference is calculated with phase_diff = $\sum^{\text{all+seasons}}|\max \text{phase}_{\text{parameter}} - \max \text{phase}_{\text{carnegie}}| + \sum^{\text{all+seasons}}|\min \text{phase}_{\text{parameter}} - \min \text{phase}_{\text{carnegie}}|$ and total amplitude difference is calculated with amp_diff = $\sum^{\text{all+seasons}}|\text{amplitude}_{\text{parameter}} - \text{amplitude}_{\text{carnegie}}|$.

Parameters	Maximum phase (UTC)					Minimum phase (UTC)					Amplitude (max − min)/mean					Phase diff (h)	Amp diff
	All	DJF	MAM	JJA	SON	All	DJF	MAM	JJA	SON	All	DJF	MAM	JJA	SON		
Electric field Carnegie (Fig. 1)	18	19	20	21	20	2	4	4	5	4	0.35	0.56	0.34	0.33	0.49	0	0
Flash counts (Figs. 1 and 9)	17	20	17	21	17	4	3	4	5	5	0.78	0.82	0.88	0.86	0.91	12	2.19
Total rainfall (Fig. 4)	18	20	18	19	20	3	8	2	3	5	0.15	0.17	0.23	0.15	0.16	15	1.2
Oceanic rainfall (Fig. 4)	18	20	18	18	20	7	8	7	3	5	0.1	0.15	0.16	0.11	0.12	21	1.42
Land rainfall (Figs. 4 and 9)	19	18	18	20	20	2	2	2	3	3	0.36	0.5	0.47	0.34	0.35	12	0.36
Thunderstorm rainfall (Figs. 5 and 10)	19	19	18	22	20	3	3	2	5	5	0.28	0.38	0.36	0.27	0.31	9	0.51
Electrified shower rainfall (Figs. 6 and 11)	18	16	18	19	18	5	3	4	3	5	0.25	0.41	0.37	0.24	0.33	16	0.54

Carnegie curve and a good match of maximum amplitude at 1900 UTC and the minimum at 0300 UTC. The diurnal variation of thunderstorm rainfall over land has appreciably higher amplitude (>40% peak to peak) and over ocean has appreciably lower amplitude (<20% peak to peak) than the Carnegie curve (~30% peak to peak).

The diurnal variations of rainfall from electrified shower clouds in universal time are shown in Fig. 6. Although the sampling noise from electrified shower clouds should be similar to that from thunderstorms, we note that the curves in Fig. 6 are not as smooth.

The maximum of rainfall from electrified shower clouds is at 1800 UTC and the minimum of the rainfall from electrified shower clouds is too noisy to determine closely. In general, the agreement with the Carnegie curve for rainfall from electrified shower clouds alone is substantially worse than the comparisons with rainfall (Fig. 4) and with thunderstorm rainfall (Fig. 5).

The diurnal variation of the rainfall contribution from thunderstorms and electrified shower clouds in universal time is shown in Fig. 7a. There is a slight (~4%) diurnal variation of the rainfall contribution from thunderstorms, with a maximum when the Americas are most convectively active and a minimum when the sun is over the Pacific Ocean. The electrified shower clouds show an almost constant rainfall contribution in universal time. The diurnal variation of the total rainfall yield per flash in universal time (Fig. 7b) has a surprisingly strong cycle. Because the thunderstorm rainfall during 0300–0600 UTC is mainly from the Maritime Continent and during 1500–2000 UTC is mainly from the Americas, this is consistent with lower flash rates per storm (higher rainfall yield per flash) over the Maritime Continent, characteristic of a more ''oceanic'' convective storm population. In contrast, Africa is the most continental tropical region (Williams and Sátori 2004; Williams 2005), and the minimum rainfall yield per flash is noted in Fig. 7b when Africa is most convectively active at 1400–1500 UTC.

c. *Seasonal variation of diurnal cycles of electric field*

The major features of the seasonal variation of the global electrical circuit are well established (Adlerman and Williams 1996; Burns et al. 2005; Markson 2007). It is useful to compare the diurnal variations of quantities of interest to the Carnegie curve during different seasons. Here we utilize the observations of fair weather electric field in different seasons at Vostok, Antarctica, (Burns et al. 2005) as a basis for comparison. (Observations of ionospheric potential with season would be preferable for this comparison, but such data do not exist.) A tendency is evident for a delayed maximum in these ''Carnegie curves'' in NH summer (compared to NH winter) because of the shapes of tropical continental landmasses. The longitudinal centroids of the landmasses shift westward in the NH summer, and this manifests itself as a delay in universal time. In general, these diurnal variations have phases and amplitudes consistent with the surface electric field at Vostok.

The diurnal variations of flash counts measured by TRMM LIS during different seasons are shown with that from the Vostok electric field in Fig. 8. Consistent with earlier studies (e.g., Williams and Heckman 1993; Bailey

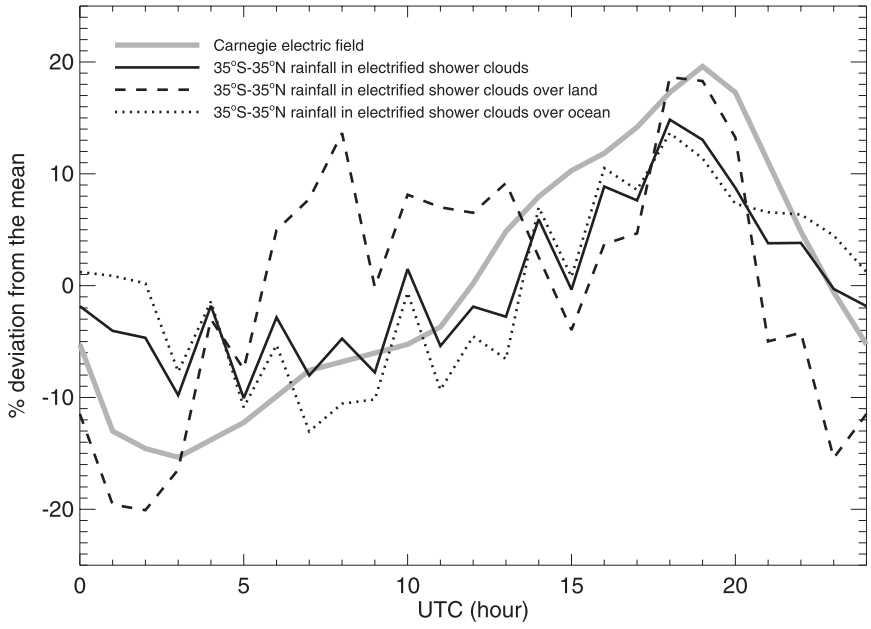

FIG. 6. As in Fig. 4 but for electrified shower clouds.

et al. 2006, 2007), the diurnal variation of global lightning shows a factor of 2 larger amplitude variation than that of the surface electric field at Vostok in all seasons. There is also a phase difference most pronounced during March–May between the Vostok curve and lightning, which is mainly driven by the dominance of the lightning in Africa (Fig. 8b).

Given the good consistency between the diurnal variation of rainfall over land and the Carnegie curve (Fig. 4), it is interesting to show the diurnal variations of rainfall over land in all four seasons (Fig. 9). For comparison with the diurnal variations of flash counts in Fig. 8, rainfall over land closely follows the amplitude of the Vostok electric field. A different minimum in the electric field is evident during December–February. The higher diurnal variation during 0300–0900 UTC in comparison with the electric field is mainly driven by inclusion of some non-electrified rainfall over the Maritime Continent.

The diurnal variations of thunderstorm rainfall in four seasons are shown in Fig. 10. The only obvious difference is the wrong phase at minimum amplitude during December–February (Fig. 10a). This may be partially caused by the lower quality of the electric field over Vostok owing to the contamination of weather and the temperature changes in this season (Burns et al. 2005). Note that, even though the proportional contribution from thunderstorms over different regions varies seasonally, the domination of one region is never as obvious with thunderstorm rainfall as with the lightning in Fig. 9 and the earlier results on thunder days (Whipple and Scrase 1936).

Figure 11 shows the diurnal variation of rainfall from electrified shower clouds. The African contribution is lower than the American contribution in all seasons, but the overall amplitude variations are generally weaker than that of the Carnegie curve.

d. Discussion

The maximum and minimum phases, amplitudes of the Carnegie curve, diurnal variations of the Vostok surface electric field, flash counts, rainfall from all PFs, thunderstorms, and electrified shower clouds are summarized in Table 2. Among all candidates, two quantities stand

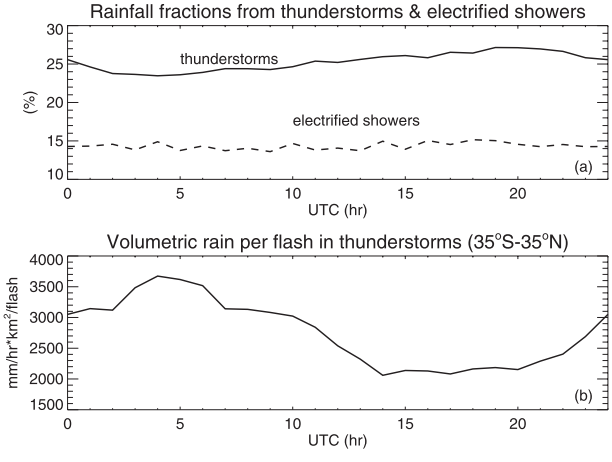

FIG. 7. (a) Fraction of rainfall from thunderstorms and electrified shower clouds from 35°S to 35°N. (b) Volumetric rainfall per flash in thunderstorms.

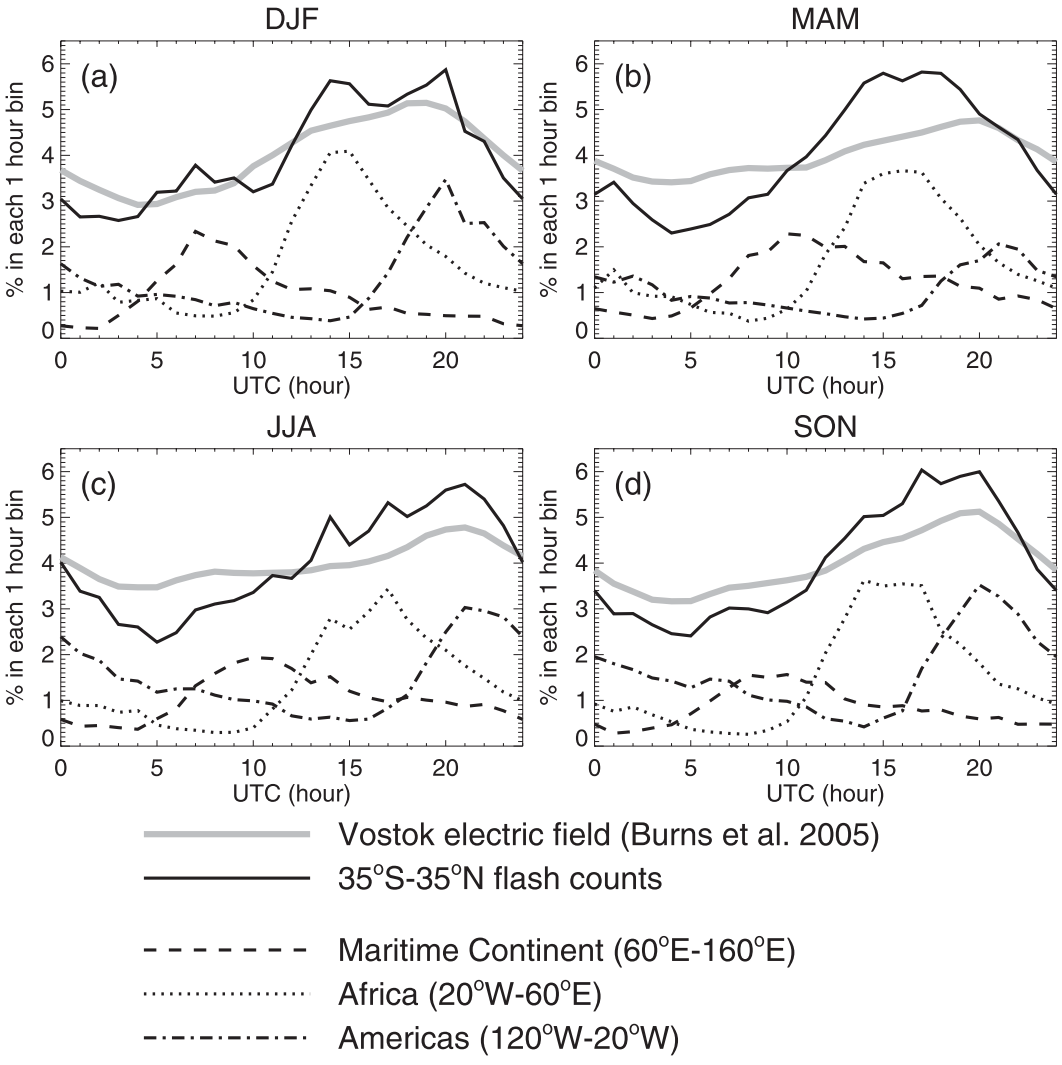

FIG. 8. Seasonal variations of diurnal variations of surface electric field over the Antarctic Vostok station (Burns et al. 2005) and LIS flash counts over tropics and subtropics. The diurnal variations of flash counts from over three longitudinal zones between 35°S and 35°N are also shown for (a) December–February, (b) March–May, (c) June–August, and (d) September–November.

out as representing the Carnegie curve reasonably accurately in both amplitude and phase: the rainfall over land (best amplitude agreement) and the thunderstorm rainfall (best phase agreement).

The diurnal curve for rainfall over land (Fig. 4), which includes rainfall contributions from electrified shower clouds and thunderstorms, shows excellent agreement with the Carnegie curve at its maximum and minimum, but a notable positive departure is evident during the period of peak convective activity in the Maritime Continent (0500–1200 UTC) and a notable negative departure during the peak activity in Africa (1300–1700 UTC), suggesting that the electrical contribution from rainfall is inaccurately represented in the most maritime (MC) and the most continental (Africa) regions.

The behavior for thunderstorm rainfall over land (Fig. 5) is somewhat larger in amplitude variation than the Carnegie curve. Based on the behavior of electrified shower clouds in this work, the addition of the rainfall from this population of clouds would certainly dilute this amplitude variation, but we lack an accurate method for weighting the shower cloud contribution relative to that of the thunderstorms.

The other quantities tested in Table 2, most notably flash counts and total rainfall, show substantial departures from Carnegie behavior. This additional evidence in these contemporary TRMM observations that lightning is not the main source of the DC global circuit is a reminder of the mismatch between the Carnegie curve and global thunder days in Whipple's (1929) seminal work.

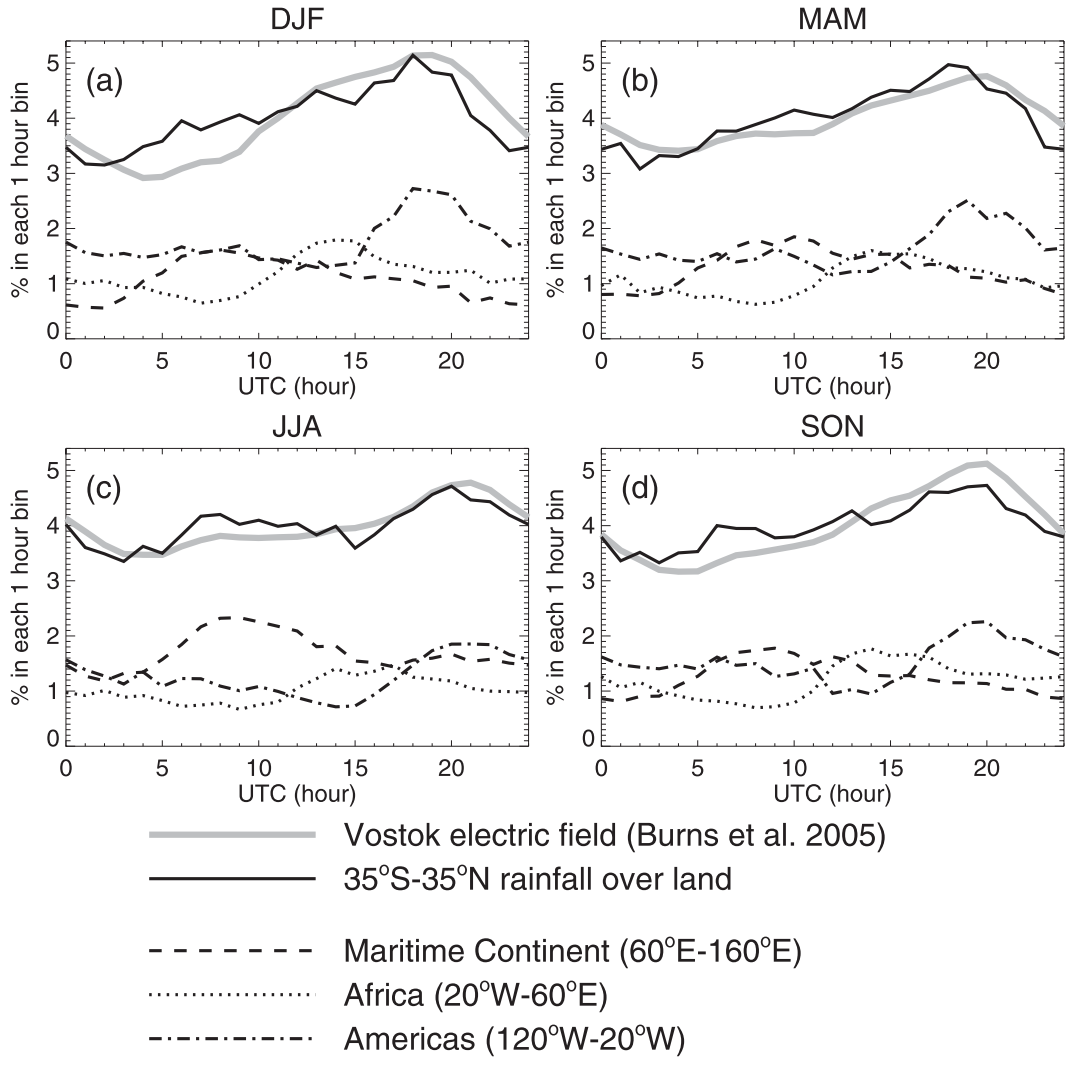

FIG. 9. As in Fig. 8 but for the Vostok station electric field and rainfall over tropical and subtropical land.

This is also a reminder that Wilson (1920) called attention to both thunderstorms and electrified shower clouds as sources for the DC global circuit.

As with thunderstorms, the electrified shower clouds follow characteristic diurnal variations in universal time over the three ''chimney'' regions in all seasons (Fig. 11), with respective maxima at roughly 0800 (MC), 1400 (Africa), and 2000 UTC (South America). However, unlike the thunderstorm populations, the relative abundances of electrified shower clouds by chimney follows a reverse order, with a maximum population in the Maritime Continent, an intermediate population in the Americas, and a minimum in Africa. The dominance of the Americas over Africa in both thunderstorm rainfall and electrified shower cloud rainfall (in contrast to lightning alone, in which Africa dominates) supports the qualitative hypothesis in Williams and Sátori (2004) for the dominance of the Americas over Africa in the Carnegie curve, with the maximum near 1900 UTC when afternoon South American storms are most active. This finding serves to resolve one of the inconsistencies set forth in Fig. 1 (and discussed further in Williams 2009), an important motivation for this study.

Two effects serve to flatten the UTC diurnal variation of electrified shower clouds (Fig. 6) relative to the Carnegie curve: 1) the frequent predominance of the Maritime Continent (among the three tropical chimneys) in electrified shower clouds and 2) the substantial populations of electrified shower clouds over tropical oceans (Fig. 3). This result is consistent with the ideas established by the NASA Marshall Space Flight Center (MSFC) in their cloud top measurements of Wilson conduction currents to the ionosphere (Mach et al. 2009), where a significant role for electrified

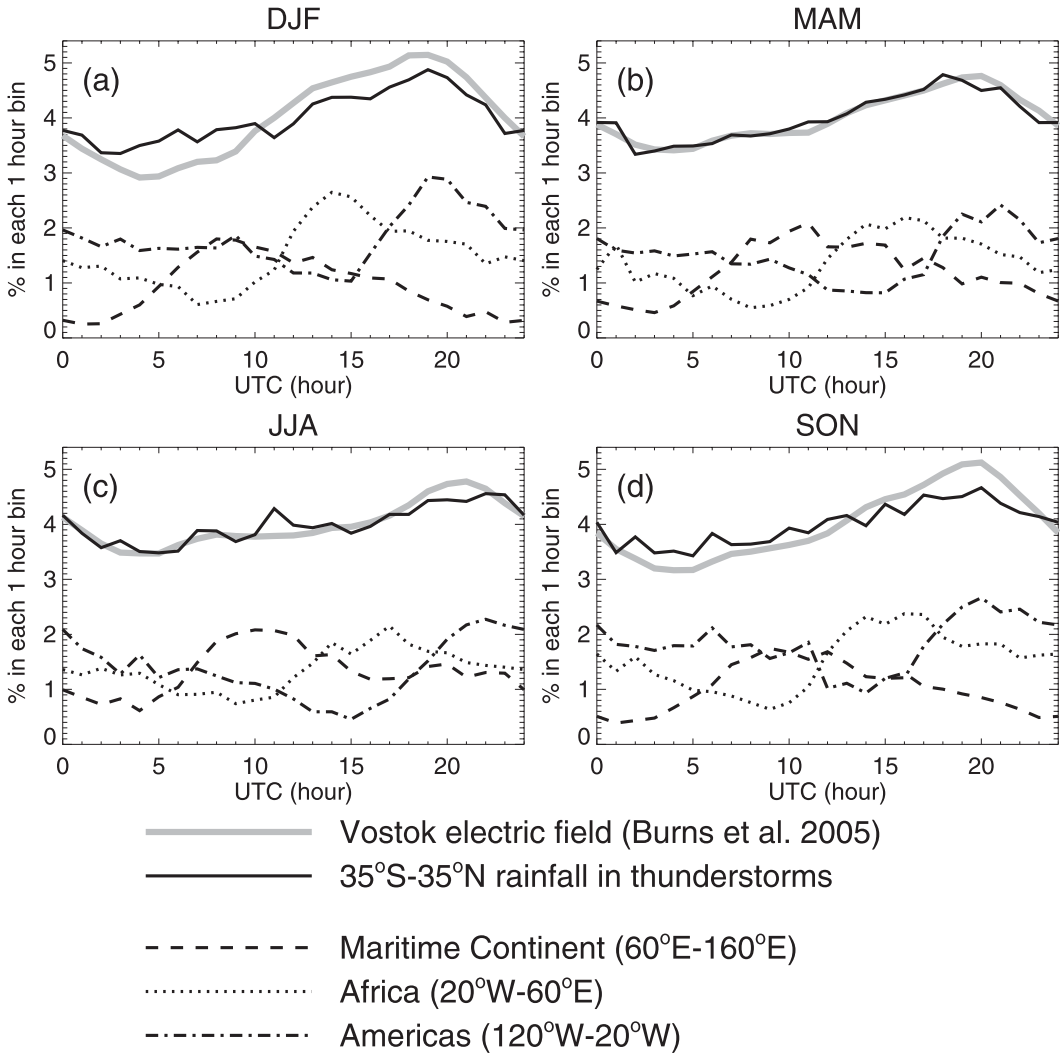

FIG. 10. As in Fig. 8 but for the Vostok station electric field and rainfall from thunderstorms.

shower clouds was also identified. The relatively flat UTC variation of electrified shower clouds (Fig. 6) plays a similar role to Whipple's (1929) guessed (but incorrect) accounting for oceanic thunderclouds (the heavy dashed curve in Fig. 1): both serve to reduce the amplitude variation of the global circuit relative to the contribution from lightning and thunderclouds alone. But a notable distinction from Whipple's guess is that the electrified shower clouds inferred from the present analysis are more prevalent over the land than over the sea.

In retrospect, although the TRMM-based PFs provide approximations to the TRMM-observed thunderstorms and electrified shower clouds that we seek to quantify, this dataset is not ideally suited to study the integrated contribution of convective storms to the global electrical circuit. The primary objective of the TRMM is obviously rainfall, and the PFs are defined as regions of contiguous radar-observed rainfall at the surface. Therefore, a modification of the TRMM PF database that specifically targets convective cells with concentrated radar reflectivity, rather than regions of contiguous rainfall at the surface, would have been better suited to the global circuit objectives laid out here.

In contrast with the mesoscale emphasis of the TRMM database used here, the principal aircraft observations of the Wilson conduction current at cloud-top level (Gish and Wait 1950; Blakeslee et al. 1989; Mach et al. 2009, 2010) have focused on the convective scale. The reason for this emphasis is partly historical in the sense that the pioneering measurements (Gish and Wait 1950) targeted big isolated thunderstorms. In more recent campaigns (Mach et al. 2009, 2010), the ER-2 pilots have generally aimed at the easily spotted deeper convective elements, given the

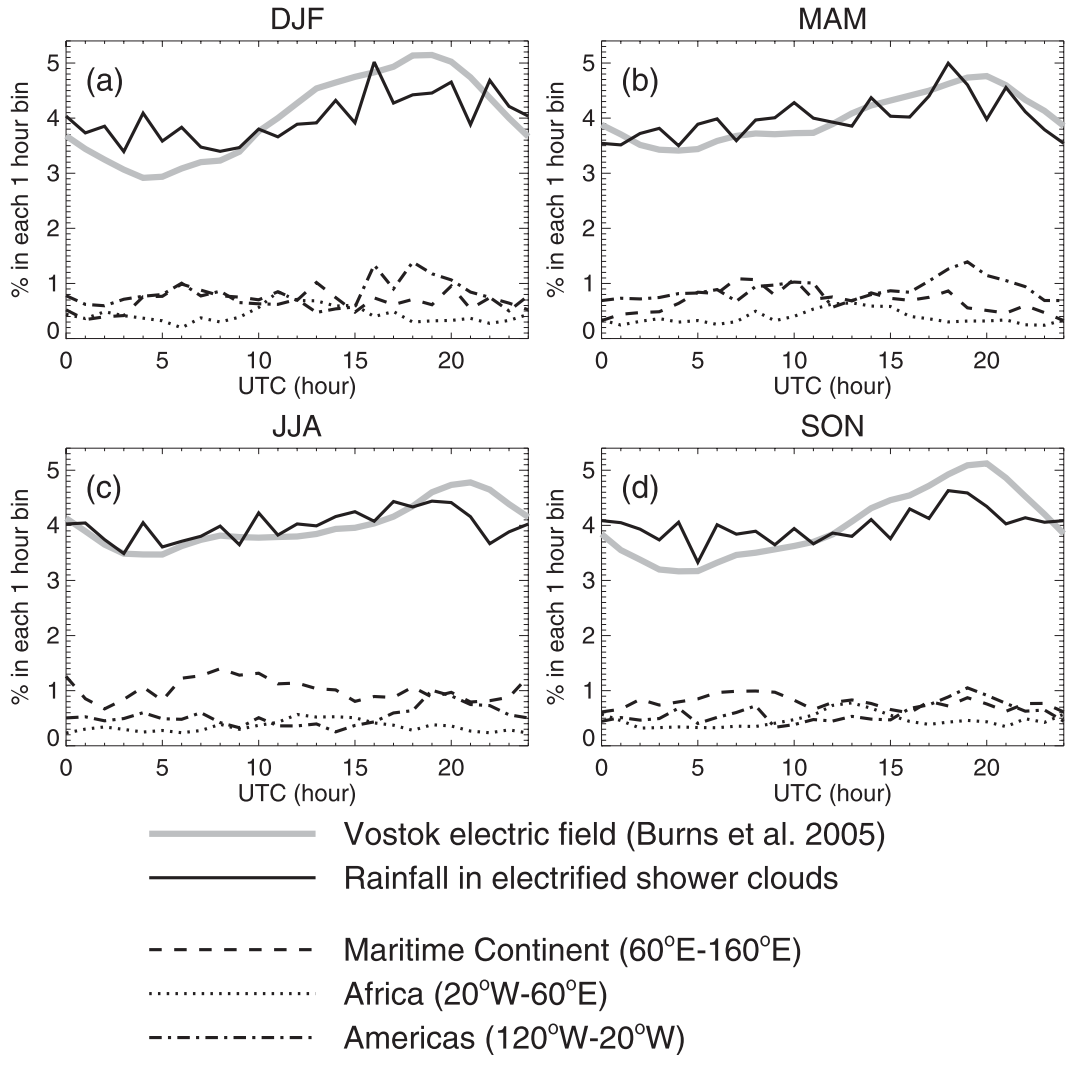

FIG. 11. As in Fig. 8 but for the Vostok station electric field and rainfall from electrified shower clouds.

empirical evidence that the strongest perturbations in electric field are found there.

One scarce but useful example of an aircraft overflight of an oceanic squall line (22 February 1993; D. Mach and R. Blakeslee 2009, personal communication, and Mach et al. 2009) sheds light on both the convective/mesoscale issue and the electrified shower clouds important for this study. The storm occurred during the Tropical Ocean Global Atmosphere Coupled Ocean–Atmosphere Response Experiment (TOGA COARE) in 1993. Aspects of the aircraft electrical measurements are discussed in Orville et al. (1997), and the radar context of the overflights is shown in Fig. 2 of Jorgensen et al. (1997). The east–west flight tracks cross both the leading deep convection and the trailing stratiform region of this predominantly north–south oriented squall line. The overflight segments (not shown) with strongest upward-directed electric field are clearly associated with strong midlevel reflectivity in the leading convection beneath the aircraft, with opposite polarity (downward electric field with reduced magnitude) over the stratiform region. The E-field reached values of 1200, 800, and 500 V m^{-1} within a few km of 30-dBZ radar echoes extending to altitudes of 8, 11, and 7 km, respectively (D. Jorgensen 2009, personal communication). The electric field record over the leading deep convection showed no indication of lightning (Orville et al. 1997) and so this convection is interpreted as the electrified shower clouds (with the same positive-dipole polarity as thunderstorms) that have been studied more thoroughly in many regions worldwide by Mach et al. (2009, 2010).

The mesoscale structure evident in the field record is broadly consistent with other well-established electrical observations of squall lines (Engholm et al. 1990; Williams

and Yair 2006). More specifically, ground flashes with negative polarity are prevalent in the leading convection, consistent with a positive-dipole structure for that convection, and ground flashes with positive polarity are most prevalent in the stratiform regions, consistent with a predominant negative-dipole structure for that region (Shepherd et al. 1996). Consistent with the observed predominance of lightning polarity is the tendency for ground-based electric fields to be upward beneath the leading convection and downward beneath the trailing stratiform region (Engholm et al. 1990; Williams and Yair 2006). To be sure, the electrical structure of squall lines can be quite complicated in comparison with the simplifications discussed here, but the tendencies in polarity are robust.

As things stand in the present study, we have a global collection of PFs, a subset of which have been characterized as thunderstorms, if at least one lightning flash is detected anywhere within the PF, or as electrified shower clouds, if no lightning is detected and at least one cell within the PF satisfies the reflectivity–temperature criteria described earlier. Given this sorting of PFs, a rough equality in the numbers of thunderstorms and electrified shower clouds was found. This result was unexpected and led us to wonder about electrified shower clouds within thunderstorm PFs that escaped identification by virtue of our classification scheme. In a hierarchical global population of convective clouds, one expects more cumulus clouds than warm rain shower clouds, more warm rain shower clouds than electrified shower clouds, more electrified shower clouds than thunderclouds, and more thunderclouds than giant supercells with strongly overshooting tops. Some evidence for these population trends with cloud size is found in Byers and Braham (1949).

A search tool has been constructed to examine the substructure of the TRMM PFs at the scale of convective cells, with lightning locations superimposed to identify the thunderstorm cells. In a cursory examination of the full cellular structure of 90 PFs classified as thunderstorms, the number of cells judged to be in the category of electrified shower cloud outnumbered the cells with at least one LIS-identified lightning flash thunderstorm cells by more than 2 to 1, and occasionally by 4 to 1. If the mean number of electrified rain shower cells in this population of PFs is equal to the number of thunderstorm cells in the other PF population, the total number of electrified shower clouds might be three times the number of thunderclouds. If the main cloud-top conduction current of the electrified shower cloud is 25% of a typical thunderstorm cell (1 A versus 0.25 A, Mach et al. 2010), then the integrated current for the global population of electrified shower clouds would be ~75% of the thundercloud population. This estimate is a very rough one, and further statistical studies are needed at the cell scale with the TRMM database. Nevertheless, with all things considered, it seems unlikely that the contribution of the electrified shower clouds to the global circuit will be either completely dominant or entirely negligible in comparison with the thunderstorm contribution. This result is in keeping with the predictions of Wilson (1920).

4. Conclusions

In this study, the universal diurnal variations of rainfall from thunderstorms and electrified shower clouds are compared with the Carnegie curve and with the electric field over Vostok, Antarctica. Some major conclusions are listed below.

- The diurnal variation of rainfall (over land) and (PF) thunderstorm rainfall (over land and ocean) both show amplitude and phase similar to that of the Carnegie curve. These findings are consistent with predictions by Wilson (1903) that negative charge carried down by precipitation is responsible for the maintenance of the global electrical circuit and with Wilson (1920) that both thunderstorms and electrified shower clouds are contributing to the descent of negative charge.
- Despite Africa's dominance in lightning, the manifestation of this region in the diurnal variation of the global circuit is secondary to the Americas because of the larger electrified rainfall contribution from the latter region.
- The majority of rainfall over oceans is associated with convection that is nonelectrified (Fig. 3c) according to the definitions and thresholds used here. The existence of abundant rainfall in shallow convection can be explained by weak updrafts in the vicinity of cloud base height or by the sparsity of cloud condensation nuclei in the marine boundary layer (Williams and Stanfill 2002).
- For improved understanding of the global electrical circuit, it is important to quantify the precipitation current in convective storms with different intensity and attendant vertical development. Further observations of electrical charges on precipitation above the interfering influence of the surface corona layer (Standler and Winn 1979; Williams 2009) in different types of precipitation systems are required. Such work would forge a stronger link between the radar-measured rainfall used here as a proxy for vertical charge separation.
- Despite the existence of good matches among the diurnal variations shown in this study and besides the uncertainties in the observations themselves, some ambiguities may influence the accuracy of results. 1) Using the presence of a lightning flash as the definition of the thunderstorm might include some MCSs

in the dissipation stage with a small developing cell embedded with a few flashes, but not all large volumes of stratiform rainfall can be considered electrified (Schuur and Rutledge 2000). This may occur especially frequently over tropical oceans. 2) Electrified shower clouds as individual cells may dominate over thunderstorm cells within PFs with low flash counts, leading to an undercounting of the contribution of electrified shower clouds. A full statistical analysis of TRMM data at the cell scale is needed to fully distinguish rainfall contributions from warm rain cells, electrified shower clouds, and thunderclouds. 3) The definition of electrified shower clouds is very rough. Some storms with 30-dBZ radar echo at a temperature higher than −10°C exhibit flashes in TRMM observations (Fig. 2). How to include all possible electrified shower clouds is a challenging task and is deserving of further investigation.

Acknowledgments. This research was supported by NASA Precipitation Measurement Mission Grants NAG5-13628 under the direction of Dr. Ramesh Kakar and NASA Grant NNX08AK28G under the direction of Dr. Erich Stocker. Special thanks go to John Kwiatkowski and the rest of the TRMM Science Data and Information System (TDSIS) at NASA Goddard Space Flight Center, Greenbelt, MD, for data processing assistance. Discussions on this topic with R. Blakeslee, S. Heckman, R. Holzworth, D. Mach, R. Markson, W. Petersen, D. Rosenfeld, and S. Rutledge are much appreciated. ERW's contribution to this study was supported by NASA Grant NNX07AT03G. The Vostok electric field data were collected by a Russian–Australian collaboration approved by the Russian Foundation for Basic Research (Project 98-05-65602) and the Australian Antarctic Science Advisory Committee (AAS 974).

REFERENCES

Adlerman, E. J., and E. R. Williams, 1996: Seasonal variation of the global electrical circuit. *J. Geophys. Res.,* **101,** 29 679–29 688.

Awaka, J., T. Iguchi, and K. Okamoto, 1998: Early results on rain type classification by the Tropical Rainfall Measuring Mission (TRMM) precipitation radar. *Proc. Eighth URSI Commission F Open Symp.,* Aveiro, Portugal, URSI, 143–146.

Bailey, J. C., R. J. Blakeslee, D. E. Buechler, and H. J. Christian, 2006: Diurnal lightning distributions as observed by the Optical Transient Detector (OTD) and the Lightning Imaging Sensor (LIS). *Eos, Trans. Amer. Geophys. Union,* **87,** Fall Meet. Suppl., Abstract AE33A-1050.

——, ——, ——, and ——, 2007: Diurnal lightning distributions as observed by the Optical Transient Detector (OTD) and the Lightning Imaging Sensor (LIS). *Proc. 13th Int. Conf. on Atmospheric Electricity,* Vol. II, Beijing, China, ICAE, 657–660.

Bering, E. A., A. A. Few, and J. R. Benbrook, 1998: The global electric circuit. *Phys. Today,* **51,** 24–30.

Blakeslee, R. J., H. J. Christian, and B. Vonnegut, 1989: Electrical measurements over thunderstorms. *J. Geophys. Res.,* **94,** 13 135–13 140.

Brooks, C. E. P., 1925: The distribution of thunderstorms over the globe. *Geophys. Mem. London,* **24,** 147–164.

Burns, G. B., A. V. Frank-Kamenetsky, O. A. Troshichev, E. A. Bering, and B. D. Reddell, 2005: Interannual consistency of bimonthly differences in diurnal variations of the ground-level, vertical electric field. *J. Geophys. Res.,* **110,** D10106, doi:10.1029/2004JD005469.

Byers, H. R., and R. R. Braham, 1949: *The Thunderstorm Project*. U.S. Weather Bureau, 287 pp.

Cecil, D. J., S. J. Goodman, D. J. Boccippio, E. J. Zipser, and S. W. Nesbitt, 2005: Three years of TRMM precipitation features. Part I: Radar, radiometric, and lightning characteristics. *Mon. Wea. Rev.,* **133,** 543–566.

Engholm, C. D., E. R. Williams, and R. M. Dole, 1990: Meteorological and electrical conditions associated with positive cloud-to-ground lightning. *Mon. Wea. Rev.,* **118,** 470–487.

Gish, O. H., and G. R. Wait, 1950: Thunderstorms and the earth's general electrification. *J. Geophys. Res.,* **55,** 473–484.

Hill, R. D., 1971: Spherical capacitor hypothesis for the earth's electric field. *Pure Appl. Geophys.,* **84,** 67–74.

Holzworth, R. H., and Coauthors, 2005: Balloon observations of temporal variation in the global circuit compared to global lightning activity. *Adv. Space Res.,* **36,** 2223–2228.

Iguchi, T., T. Kozu, R. Meneghini, J. Awaka, and K. Okamoto, 2000: Rain-profiling algorithm for the TRMM precipitation radar. *J. Appl. Meteor.,* **39,** 2038–2052.

Israel, H., 1973: *Fields, Charges, Currents*. Vol. II, *Atmospheric Electricity,* Israel Program for Scientific Translation, 796 pp.

Jorgensen, D. P., M. A. LeMone, and S. B. Trier, 1997: Structure and evolution of the 22 February 1993 TOGA COARE squall line: Aircraft observations of precipitation, circulation, and surface energy fluxes. *J. Atmos. Sci.,* **54,** 1961–1985.

Kartalev, M. D., M. J. Rycroft, M. Fuellekrug, V. O. Papitashvili, and V. I. Keremidarska, 2006: A possible explanation for the dominant effect of South American thunderstorms on the Carnegie curve. *J. Atmos. Solar-Terr. Phys.,* **68,** 457–468.

Kistler, R., and Coauthors, 2001: The NCEP–NCAR 50-Year Reanalysis: Monthly means CD-ROM and documentation. *Bull. Amer. Meteor. Soc.,* **82,** 247–267.

Kummerow, C., W. Barnes, T. Kozu, J. Shiue, and J. Simpson, 1998: The Tropical Rainfall Measuring Mission (TRMM) sensor package. *J. Atmos. Oceanic Technol.,* **15,** 809–817.

Liu, C., and E. Zipser, 2008: Diurnal cycles of precipitation, clouds, and lightning in the tropics from 9 years of TRMM observations. *Geophys. Res. Lett.,* **35,** L04819, doi:10.1029/2007GL032437.

——, and ——, 2009: ''Warm rain'' in the tropics: Seasonal and regional distributions based on 9 yr of TRMM data. *J. Climate,* **22,** 767–779.

——, ——, D. Cecil, S. W. Nesbitt, and S. Sherwood, 2008: A cloud and precipitation feature database from 9 years of TRMM observations. *J. Appl. Meteor. Climatol.,* **47,** 2712–2728.

Mach, D. M., R. J. Blakeslee, M. G. Bateman, and J. C. Bailey, 2009: Electric fields, conductivity, and estimated currents from aircraft overflights of electrified clouds. *J. Geophys. Res.,* **114,** D10204, doi:10.1029/2008JD011495.

——, ——, ——, and ——, 2010: Comparisons of total currents based on storm location, polarity, and flash rates derived from high altitude aircraft overflights. *J. Geophys. Res.,* in press.

Markson, R., 2007: The global circuit intensity: Its measurement and variation over the last 50 years. *Bull. Amer. Meteor. Soc.,* **88,** 223–241.

——, L. H. Ruhnke, and E. R. Williams, 1999: Global scale comparisons of simultaneous ionospheric potential measurements. *Atmos. Res.,* **51,** 315–321.

Negri, A. J., T. L. Bell, and L. Xu, 2002: Sampling of the diurnal cycle of precipitation using TRMM. *J. Atmos. Oceanic Technol.,* **19,** 1333–1344.

Nesbitt, S. W., and E. J. Zipser, 2003: The diurnal cycle of rainfall and convective intensity according to three years of TRMM measurements. *J. Climate,* **16,** 1456–1475.

Orville, R. E., and Coauthors, 1997: Lightning in the region of the TOGA COARE. *Bull. Amer. Meteor. Soc.,* **78,** 1055–1067.

Pierce, E. T., 1958: Some topics in atmospheric electricity. *Recent Advances in Atmospheric Electricity,* Pergamon, 5–16.

Schuur, T. J., and S. A. Rutledge, 2000: Electrification of stratiform regions in mesoscale convective systems. Part I: An observational comparison of symmetric and asymmetric MCSs. *J. Atmos. Sci.,* **57,** 1961–1982.

Shepherd, T. R., W. D. Rust, and T. C. Marshall, 1996: Electric fields and charges near 0°C in stratiform clouds. *Mon. Wea. Rev.,* **124,** 919–938.

Standler, R. B., and W. P. Winn, 1979: Effects of coronae on electric fields beneath thunderstorms. *Quart. J. Roy. Meteor. Soc.,* **105,** 285–302.

Wallace, J. M., and P. V. Hobbs, 1977: Chapter on thunderstorm electrification. *Atmospheric Science: An Introductory Survey,* Academic Press, 199–209.

Whipple, F. J. W., 1929: On the association of the diurnal variation of electric potential gradient in fine weather with the distribution of thunderstorms over the globe. *Quart. J. Roy. Meteor. Soc.,* **55,** 1–17.

——, and F. J. Scrase, 1936: *Point Discharge in the Electric Field of the Earth*. Geophysical Memoirs, Vol. 7, HMSO, 20 pp.

Williams, E. R., 1988: The electrification of thunderstorms. *Sci. Amer.,* **259,** 88–99.

——, 2005: Lightning and climate: A review. *Atmos. Res.,* **76,** 272–287.

——, 2009: The global electrical circuit: A review. *Atmos. Res.,* **91,** 140–152, doi:10.1016/j.atmosres.2008.05.018.

——, and S. J. Heckman, 1993: The local diurnal variation of cloud electrification and the global diurnal variation of negative charge on the earth. *J. Geophys. Res.,* **98,** 5221–5234.

——, and S. Stanfill, 2002: The physical origin of the land–ocean contrast in lightning activity. *C. R. Physique,* **3,** 1277–1292.

——, and G. Sátori, 2004: Lightning, thermodynamic and hydrological comparison of the two tropical continental chimneys. *J. Atmos. Solar-Terr. Phys.,* **66,** 1213–1231.

——, and Y. Yair, 2006: The microphysical and electrical properties of sprite-producing thunderstorms. *Sprites, Elves, and Intense Lightning Discharges,* M. Füllekrug, E. A. Mareev, and M. J. Rycroft, Eds., NATO Science Series II, Vol. 225, Springer, 57–74.

Wilson, C. T. R., 1903: Atmospheric electricity. *Nature,* **68,** 101–104.

——, 1920: Investigations on lightning discharges and on the electric field of thunderstorms. *Philos. Trans. Roy. Soc. London,* **221A,** 73–115.